International Journal of Nanomedicine

Dovepress
open access to scientific and medical research

Open Access Full Text Article

ORIGINAL RESEARCH

Fabrication of KR-12 peptide-containing hyaluronic acid immobilized fibrous eggshell membrane effectively kills multi-drug-resistant bacteria, promotes angiogenesis and accelerates re-epithelialization

This article was published in the following Dove Press journal:
International Journal of Nanomedicine

International Journal of Nanomedicine downloaded from https://www.dovepress.com/
For personal use only.

Menglong Liu[1]
Tengfei Liu[1]
Xiaorong Zhang[1]
Zhiwen Jian[2]
Hesheng Xia[2]
Jiacai Yang[1]
Xiaohong Hu[1]
Malcolm Xing[1,3]
Gaoxing Luo[1]
Jun Wu[1,4]

[1]Institute of Burn Research, State Key Laboratory of Trauma, Burn and Combined Injury, Southwest Hospital, Third Military Medical University (Army Medical University), Chongqing 400038, People's Republic of China; [2]State Key Laboratory of Polymer Materials Engineering, Polymer Research Institute of Sichuan University, Chengdu, 610065, People's Republic of China; [3]Department of Mechanical Engineering, University of Manitoba, Winnipeg, MB R3T 2N2, Canada; [4]Department of Burns, the First Affiliated Hospital, SunYat-Sen University, Guangzhou 510080, People's Republic of China

Correspondence: Malcolm Xing; Jun Wu
Institute of Burn Research, State Key Laboratory of Trauma, Burn and Combined Injury, Southwest Hospital, Third Military Medical University (Army Medical University), 30 Gaotanyan Street, Shapingba District, Chongqing 400038, People's Republic of China
Email malcolm.xing@umanitoba.ca; editorinchief@burninchina.com

Background: Designing a wound dressing that effectively prevents multi-drug-resistant bacterial infection and promotes angiogenesis and re-epithelialization is of great significance for wound management.

Methods and results: In this study, a biocompatible composite membrane comprising biomimetic polydopamine-modified eggshell membrane nano/microfibres coated with KR-12 antimicrobial peptide and hyaluronic acid (HA) was developed in an eco-friendly manner. The physicochemical properties of the composite membrane were thoroughly characterized, and the results showed that the surface hydrophilicity and water absorption ability of the composite membrane were improved after the successive conjugation of the HA and the KR-12 peptide. Furthermore, the in vitrobiological results revealed that the composite membrane had excellent antibacterial activity against Gram-positive *Staphylococcus aureus*, methicillin-resistant *Staphylococcus aureus* (MRSA) and Gram-negative *Escherichia coli*, and it could prevent MRSA biofilm formation on its surface. Additionally, it promoted the proliferation of keratinocytes and human umbilical vein endothelial cells and increased the secretion of VEGF. Finally, an in vivo animal study indicated that the composite membrane could promote wound healing via accelerating angiogenesis and re-epithelialization, which were demonstrated by the enhanced expression of angiogenetic markers (CD31 and VEGF) and keratinocyte proliferation marker (PCNA), respectively.

Conclusion: These results indicated that the composite membrane is a potential candidate of wound dressings

Keywords: antimicrobial peptides, hyaluronic acid, fibrous eggshell membrane, antibacterial activity, angiogenesis, re-epithelialization

Introduction

A cutaneous wound is typically protected with a dressing to enhance the rate and quality of healing.[1] An ideal wound dressing should possess the capacity to effectively protect the wound from bacterial infection, promote angiogenesis and accelerate the re-

© 2019 Liu et al. This work is published and licensed by Dove Medical Press Limited. The full terms of this license are available at https://www.dovepress.com/terms.php and incorporate the Creative Commons Attribution – Non Commercial (unported, v3.0) License (http://creativecommons.org/licenses/by-nc/3.0/). By accessing the work you hereby accept the Terms. Non-commercial uses of the work are permitted without any further permission from Dove Medical Press Limited, provided the work is properly attributed. For permission for commercial use of this work, please see paragraphs 4.2 and 5 of our Terms (https://www.dovepress.com/terms.php).

epithelialization process.[2,3,4] Additionally, a dressing should have a suitable porous structure for water and gas exchange and wound exudate absorption.[3,5] However, the demand of such multi-functionality for a wound dressing remains a challenge.

Antibiotics such as gentamicin and amoxicillin are generally grafted onto wound dressings to provide antibacterial activity.[6,7] However, the increasing emergence of antibiotic-resistant bacteria has become one of the largest threats to public health, as declared by the WHO in 2014.[8] Therefore, it is urgent to find alternatives to antibiotics. Functional peptides have been widely used in biomedical sciences, such as cancer therapy and antibacterial therapy in recent years.[9,10,11] Particularly, antimicrobial peptides (AMPs) have attracted great attention as an antibacterial agent.[11,12,13] As a natural immune defence, AMPs are secreted by animals, plants and even some microorganisms, and they have shown remarkable broad-spectrum antibacterial activity.[11,14] It is widely believed that cationic AMPs could target the bacterial surface via the electrostatic attraction between positively charged amino acids and the negatively charged cell surface and destroy bacteria by physically disrupting the bacterial cell membrane.[15,16] This particular mechanism of action makes AMPs seldom induce drug resistance. The KR-12 peptide, which is identified as the smallest antibacterial motif (residues 18–29) of human cathelicidin LL-37, displays potent antibacterial activity against both Gram-negative bacteria and Gram-positive bacteria, including methicillin-resistant *Staphylococcus aureus* (MRSA).[17,18] Apart from antibacterial activity, KR-12 peptide was reported to modulate inflammation and accelerate the re-epithelialization process via promoting keratinocyte proliferation and migration.[19,20] The potential cytotoxicity and hemolysis of free KR-12 and LL-37 narrow their applications, but it has been reported that immobilizing them on materials relieves this concern.[18,21] Thus, because of the fascinating advantages, KR-12 peptide is a valuable antibacterial candidate to include in the fabrication of wound dressings.

In addition to the inhibition of bacterial infection and promotion of re-epithelialization, angiogenesis is another important issue during the wound healing process because the newly generated blood vessels can transport nutrients and growth factors for tissue formation.[4,22] Hyaluronic acid (HA) is a natural linear polysaccharide mainly found in hydrated tissues, such as the eye, cartilage, bone and skin.[23,24] It is composed of repeated disaccharides of β-1,4-linked D-glucuronic acid and β-1,3-linked N-acetyl-D-glucosamine and displays unique biological properties, such as biodegradability, biocompatibility, hydrophilicity and water control ability.[25,26] As an essential component of the skin extracellular matrix, HA has been demonstrated to be beneficial for rapid wound healing.[27,28] More noteworthy, accumulating evidence in recent years has indicated that HA plays an important role in modulating angiogenesis via promoting the proliferation of endothelial cells and secretion of angiogenesis-related cytokines.[29,30,31,32] Thus, the immobilization of HA into a wound dressing is helpful for angiogenesis in the wound healing process.

The eggshell membrane (ESM) is a fibrous connective tissue between the egg white and eggshell. As a natural biomaterial, ESM is biocompatible with human cells and easy to obtain at low cost.[33] ESM possesses a three-dimensional fibrous meshwork structure, and its nano/microfibres are mainly made up of proteins (80–85%).[34] The characteristic porous meshwork structure provides ESM with a large surface area for biomolecule deposition and suitable porosity for gas and water exchange, which are essential factors for wound dressings.[33,35] Furthermore, ESM has been well demonstrated to be beneficial to fibroblast proliferation and wound healing.[36,37] These features make ESM a good scaffold for wound dressings.

In this study, a biocompatible composite membrane composed of biomimetic polydopamine-modified ESM nano/microfibres coated with KR-12 peptide and HA (ESM/KR-12) was prepared using a three-step approach (Figure 1A). First, the ESM was modified with a biomimetic polydopamine, which contains multiple active groups and possesses strong adhesive capacity.[38,39] Second, HA was immobilized on the polydopamine coating via chemical/physical interactions. Third, because HA is negatively charged while KR-12 is positively charged, the KR-12 peptide was conjugated onto the HA coating via electrostatic interaction in a facile manner.[18,40] The whole fabrication process was carried out in an eco-friendly way at room temperature. We hypothesize that the ESM/KR-12 composite membrane has antibacterial properties, including the capacity to kill multi-drug-resistant bacteria, and can promote angiogenesis and re-epithelialization, leading to rapid wound healing.

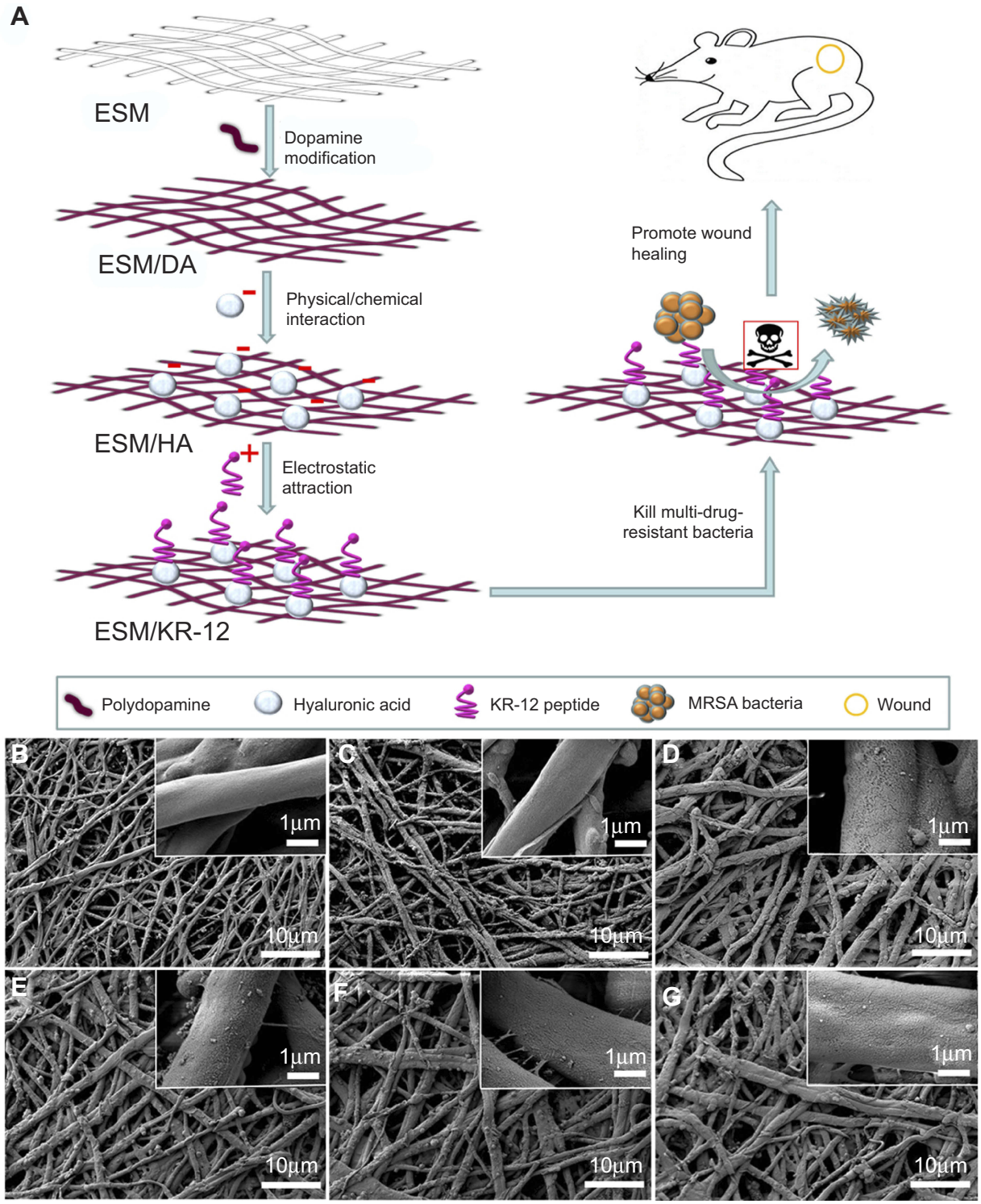

Figure 1 (**A**) Schematic of the preparation and biological effects of ESM/KR-12 membrane. SEM images of (**B**) ESM, (**C**) ESM/DA, (**D**) ESM/HA, (**E**) ESM/KR_{300}, (**F**) ESM/KR_{600} and (**G**) ESM/KR_{900} membranes.
Abbreviations: ESM, eggshell membrane; HA, hyaluronic acid.

Materials and methods

Materials and animals

Fresh eggs were obtained from a supermarket (Chongqing, People'sRepublic of China). Dopamine (DA) hydrochloride, sodium salt of HA (~2000 kDa) and 5, 5′-dithiobis-(2-nitrobenzoic acid) (DTNB) were purchased from Solarbio Science & Technology (Beijing, People's Republic of China). Analogue-3 of the original KR-12 peptide

(CKRIVKRIKKWLR, >95% purity) was obtained from Sangon (Shanghai, People's Republic of China).[18,20] *Staphylococcus aureus* (*S. aureus*, ATCC 25923), MRSA (ATCC 43300) and *Escherichia coli* (*E. coli*, ATCC 25922) were obtained from Clinical Microbiology Laboratory, Southwest Hospital (Chongqing, People's Republic of China).

BALB/c mice (female, ~25 g, 12 weeks old, specific pathogen-free level) were purchased from the Animal Department of Third Military Medical University (TMMU). All animal experimental methods were approved by the ethical committee of TMMU, and all animal tests were performed in accordance with the guidelines of TMMU.

Preparation of ESM/KR-12 composite membranes

The ESM was carefully peeled from fresh eggshells using forceps and washed three times with deionized water. Next, the ESM was immersed into a DA solution (2 mg/mL in 10 mM Tris-HCl, pH=8.5) for 16 hrs. After rinsing twice with deionized water, the DA-coated ESM was immersed into a sodium HA aqueous solution (4 mg/mL, pH=6.0) for 4 hrs. Next, the HA was adhered on the DA coating via chemical/physical combinations. After washing twice with 0.15 M NaCl aqueous solution, the HA-treated ESM was dipped into different concentrations of KR-12 solution (300, 600 and 900 μg/mL) in PBS (pH=7.4) for 40 mins to conjugate the peptide via charge attraction. Finally, the membrane was washed with deionized water and harvested for subsequent experiments. The whole process of preparation was conducted at room temperature. Subsequently, the DA-treated ESM, HA-treated ESM and KR-12-treated ESM were designated as ESM/DA, ESM/HA and ESM/KR-12 (ESM/KR_{300}, ESM/KR_{600} and ESM/KR_{900}) membranes, respectively.

Characterization of ESM/KR-12 membranes

The membrane morphology was observed under a scanning electron microscope (SEM; Crossbeam 340, Zeiss, Germany). The average porosity and fiber diameter of the membranes was analyzed using ImageJ software based on SEM images. Surface zeta potential measurement was performed by Zetasizer Nano ZSP (Malvern, UK) at room temperature. The water contact angle of the membrane was detected using a contact angle measurement instrument (Theta Lite 101; Biolin Scientific, Sweden). Attenuated total reflectance Fourier transform-infrared (ATR-FTIR) spectra were determined using an ATR-FTIR spectrometer (Nicolet 460, USA).

The loading amount of KR-12 was explored using the Ellman's assay, which was based on the absorbance alteration of the solution via the reaction between DTNB and the thiol group of KR-12.[20] Briefly, 50 μL of KR-12 solution and 150 μL of DTNB were added into a 96-well plate and incubated in the dark for 15 mins at room temperature. Next, the absorbance value of the solution was measured at 412 nm using a microplate absorbance reader (Thermo Scientific, USA). The loading ratio and loading density were calculated using the following formula:

$$\text{Loading ratio}\,(\%)=(C_1-C_2)/C_1\times 100\%,$$

$$\text{Loading density}=(C_1-C_2)\times V/S,$$

where C_1 and C_2 represent the concentrations of KR-12 solution before and after peptide coating, respectively, V represents the volume of KR-12 solution, and S represents the surface area of the membrane.

To measure the swelling percentage, a piece of membrane (10×10 mm) was immersed in PBS (pH=7.4) for various times (0.5–24 hrs) at 37°C, and the membrane was weighed before and after swelling. The swelling percentage (%) of the membrane was calculated using the following formula:

$$\text{Swelling percentage}\,(\%)=(W_s-W_i)/W_i,$$

where W_s is the weight of membrane after a certain swelling time and W_i is the weight of the membrane in the dry state.

Antibacterial test

The antibacterial activity of the membrane was assessed against Gram-negative *E. coli*, Gram-positive *S. aureus* and MRSA. Briefly, a log-phase bacterial suspension was first diluted with Luria–Bertani (LB) medium to the initial concentration (1×10^6 colony forming units (CFU)/mL). Next, 100 μL of bacterial suspension was inoculated on the surface of membrane and incubated for 4 hrs at 37°C. After gently washing with PBS for 1 min, the sample was placed in a 24-well plate with 1 mL of PBS, followed by sonication for 10 mins. The solution was then diluted with PBS for 200×, and 25 μL of solution was uniformly spread on an agar plate. After incubation for 18 hrs at 37°C, the number of bacterial colonies was counted, and the

bacterial survival rates in different groups were calculated by comparison with the pristine ESM group.

To investigate the effect of KR-12-conjugated ESM on biofilm formation, a piece of sample was co-incubated with 300 μL of bacterial suspension (1×10^6 CFU/mL) in LB medium for 24 hrs at 37°C. Next, the sample was collected and gently rinsed twice with PBS. For SEM analysis, the sample was fixed in 4% formaldehyde, dehydrated with an ethanol solution and sputter-coated with gold. The area of biofilm was then measured using IPP 6.0 software based on SEM images as reported previously.[41] For the Live/Dead staining assay, the sample was stained by a Live/Dead staining kit (Invitrogen, USA) in the dark for 15 mins. After rinsing twice with PBS, the biofilm was observed using a fluorescence microscope (Olympus, Japan). The green signal indicated living bacteria, while the red signal indicated dead bacteria.

Cell culture and cell proliferation test

Human umbilical vein endothelial cells (HUVECs) and human keratinocytes (HaCaT) were purchased commercially from American Type Culture Collection, and cultured in DMEM supplemented with 10% FBS. Before the cell experiment, the sterilized samples were cut into small disks (diameter: 6 mm) and placed in a 96-well plate. Next, 2,500 HUVECs or HaCaT cells were seeded on each sample and incubated in an incubator at 37°C and 5% CO_2. To detect the cell proliferation level, the CCK8 assay was conducted at day 1, 3 and 5 post-seeding. Briefly, the culture medium in each well was replaced with 100 μL of fresh medium and 10 μL of CCK8 solution and then was incubated for 2 hrs at 37°C. Next, the optical density of solution at 450 nm was measured using a microplate absorbance reader (Thermo Scientific, USA). Moreover, to observe the cell morphology, the samples after 5 days of incubation were fixed in 4% formaldehyde for 0.5 hr and then were successively stained with phalloidin (100 ng/mL; Thermo Scientific) and DAPI (Thermo Scientific), which labelled F-actin (red) and the nuclei (blue) of cells, respectively. Fluorescence images of HUVECs and HaCaT cells were obtained using a fluorescence microscope (Olympus, Japan).

ELISA for vascular endothelial growth factor (VEGF) secretion

To quantify the amount of (VEGF secreted from HUVECs, the cell culture medium of each well was harvested at day 5 post-seeding. Next, the VEGF concentration was detected using an ELISA kit (Dakewe Biotech Co., Ltd, Shenzhen, People'sRepublic of China) according to the manufacturer's instructions. The results were expressed as the mass (pg) of VEGF per milliliter of culture medium.

Hemolysis assay

The hemocompatibility of the membrane was evaluated using a hemolysis assay as described previously.[42] Human whole blood (diluted 10-fold with normal saline) was obtained from Southwest Hospital, Chongqing, People'sRepublic of China. All studies involving human whole blood were approved by the ethics committee of first affiliated hospital of TMMU and performed in accordance with the institutional and international guidelines. Written informed consent has been provided by the donors in compliance with the Declaration of Helsinki. Prior to the assay, each sample was cut into a rectangular strip (10×25 mm) and was incubated in 10 mL of normal saline at 37°C for 1 hr. Next, 200 μL of diluted blood was added and incubated for another 1 hr at 37°C. Finally, the solution was centrifuged at 3000 rpm for 5 mins at room temperature, and the absorbance of supernatant fluid at 545 nm was measured using a microplate absorbance reader (Thermo Scientific). Here, the deionized water mixed with blood served as a positive control group, while the normal saline mixed with blood served as a negative control group. The hemolysis ratio (HR) was calculated according to the following formula:

$$HR\,(\%)=(A_M-A_N)/(A_P-A_N)\times100\%,$$

where A_M represents the absorbance of blood treated with the membrane, A_P represents the absorbance of blood treated with deionized water and A_N represents the absorbance of blood treated with normal saline.

In vivo animal test

A murine skin wound model (five mice per group) was conducted for the in vivo test as previously described.[43] The mice were anesthetized with 1% pentobarbital via intraperitoneal injection, and the dorsal hairs were shaved. Next, two full-thickness wounds (diameter: 6 mm) were created on either side of the back using a punch. After being photographed by a digital camera, the wounds were immediately covered by ESM, ESM/DA, ESM/HA or ESM/KR_{600} membranes and were kept in place by an adhesive bandage. The wounds that only covered with an adhesive bandage were served as the control group. At days 2, 4 and 8, the wounds were photographed, and the dressings were replaced. Based on the photographs, the wound areas were carefully measured using IPP 6.0 software by two independent

researchers. The reserved wound area at a certain time point was calculated using the following formula:

$$\text{Percentage of wound area}\,(\%) = R/I \times 100\%,$$

where R represents the number of pixels of the reserved wound area at a certain time point, while I represents the number of pixels of the initial wound area.

Furthermore, to determine the average wound closure times, five additional mice in every group were observed until the wounds were completely closed.

Histological examination

The mice were sacrificed at day eight post-surgery, and then the wound tissues with adjacent normal skin (10×10 mm) were carefully harvested and fixed in 4% paraformaldehyde for 24 hrs. Next, the tissues were embedded in paraffin and sliced at a thickness of 5 μm. H&E staining was performed for histological analysis. The number of inflammatory cells in the wound edge, thickness of granulation tissue and length of regenerated epidermis, which was defined as the distance from the border between normal skin and wound region to the anterior edges of newly generated epidermis,[43] were quantified using ImageJ software by two independent researchers.

Immunohistochemistry analysis

Immunohistochemistry analysis was conducted as previously described.[3] Briefly, wound tissue sections were deparaffinized, rehydrated and boiled in a 100°C citrate buffer bath. Next, the sections were treated with primary antibodies at 4°C overnight. The primary antibodies obtained from Abcam (UK) were as follows: anti-CD31 (cluster of differentiation 31) antibody at 1:250 dilution, ab28364; anti-PCNA (proliferating cell nuclear antigen) antibody at 1:200 dilution, ab15497; and anti-VEGF antibody at 1:200 dilution, ab46154. After incubation with goat-anti-rabbit IgG antibody and avidin-peroxidase reagent, the sections were stained with 3,30-diaminobenzidine tetrahydrochloride (DAB) solution and hematoxylin and then were photographed under a microscope (CTR6000, Leica, Germany). Based on the images, the number of PCNA-positive keratinocytes per field, the number of CD31-positive blood vessels per field and relative intensity of VEGF protein (compared with control group) were counted and analyzed using ImageJ software by two independent researchers.

Statistical analysis

The data were expressed as the mean±SD, and the results were analyzed by one-way ANOVA. $P<0.05$ was considered statistically significant.

Results and discussion

Characterizations of composite membranes

The composite membranes were first characterized by SEM. As shown in Figure 1B, pristine ESM exhibited a three-dimensional network structure consisting of interwoven nano/microfibres and hollow spaces. The diameter of fibers ranged from 0.5 to 2.0 μm, and the fiber surface was smooth. After being coated with polydopamine, the ESM/DA fiber was slightly rougher than that of the ESM (Figure 1C), but no obvious difference was found in the morphology between the ESM and the ESM/DA. Figure 1D shows the microscopic feature of the ESM coated by HA. The ESM/HA still maintained a fibrous network structure, but a homogeneous layer with aggregations was apparent on the fiber surface. Moreover, compared with the ESM/DA, the average fiber diameter of the ESM/HA measured by ImageJ software was significantly increased from 1.37 to 1.72 μm (Table 1). Correspondingly, the porosity of the ESM/HA was decreased from 44.09% to 42.05%. The overall results suggested that HA was successfully grafted on the polydopamine-modified ESM scaffold. Polydopamine possesses strong adhesive capacity, and its catechol group could react with various biomolecules under physiological conditions; thus, we assumed that HA was immobilized on the polydopamine coating via physical/chemical interactions.[38,39] The morphologies of the ESM/KR_{300}, the ESM/KR_{600} and the ESM/KR_{900} presented in Figure 1E-G were similar to that

Table 1 Porosities and fibre diameters of ESM, ESM/DA, ESM/HA, ESM/KR_{300}, ESM/KR_{600} and ESM/KR_{900} membranes

	ESM	ESM/DA	ESM/HA	ESM/KR_{300}	ESM/KR_{600}	ESM/KR_{900}
Porosity (%)	44.31±5.92	44.09±5.06	42.05±4.57	41.53±5.88	41.25±3.79	41.04±4.37
Fibre diameter (μm)	1.23±0.50	1.37±0.55	1.72±0.48	1.77±0.43	1.79±0.42	1.80±0.47

Abbreviations: ESM,eggshell membrane;HA,hyaluronic acid.

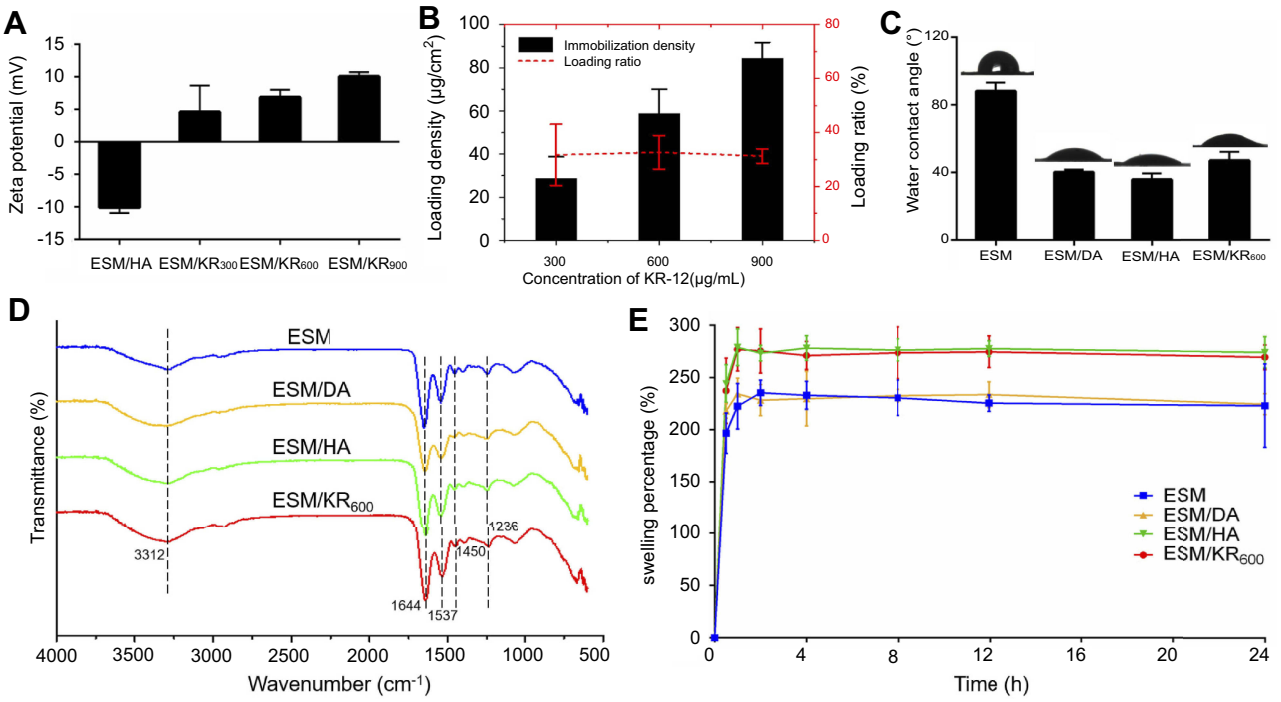

Figure 2 Characterizations of the composite membranes (n=3). (**A**) Zeta potentials of ESM coated with HA and ESM coated with different concentrations of KR-12 peptide. (**B**) Loading density and loading ratio of KR-12 peptide on ESM. (**C**) Water contact angles of pristine ESM and composite membranes. (**D**) ATR-FTIR spectra of pristine ESM and composite membranes. (**E**) Swelling percentages of pristine ESM and composite membranes.
Abbreviations: ESM, eggshell membrane; HA, hyaluronic acid.

of the ESM/HA, and the cause might be because that the nanosized peptide layer was too thin to distinguish.[44]

Figure 2A shows the alteration sign of the zeta potential along with the successive deposition of HA and KR-12 peptide. As previously described, the surface of HA coating exhibited a negative zeta potential.[40] However, after treatment with KR-12 solutions, the surface zeta potential became clearly positive, and the charge was enhanced with the concentration increase of KR-12 peptide. This result suggested that positively charged KR-12 was deposited on the negatively charged HA coating via electrostatic attraction.[18,40] To determine the loading amount of KR-12 peptide on the ESM scaffold, Ellman's assay was conducted. As shown in Figure 2B, the loading densities of KR-12 on the ESM/KR_{300}, the ESM/KR_{600} and the ESM/KR_{900} membranes were 28.5, 58.8 and 84.4 μg/mL, respectively, which were proportional to the concentration of KR-12 solution in the reaction medium. The loading ratios of the three membranes were all approximately 32.0%, likely because the loading efficacy was not influenced by the concentration of KR-12 peptide.

Figure 2C shows the water contact angles of the ESM, the ESM/DA, the ESM/HA and the ESM/KR_{600} membranes. After being coated with polydopamine, the contact angles of ESM/DA were significantly decreased from 88.2° to 40.2°, due to the super hydrophilic property of the polydopamine layer.[45] Similarly, the subsequent immobilized HA coating kept the membrane surface hydrophilic. The water contact angle of the ESM/KR_{600} was slightly increased to 47.1°, which is likely attributed to the hydrophobic residue of KR-12 present on the membrane surface.[17,46] As the surface wettability influenced the biological behaviours of the biomaterial, we speculated that such an improvement in the surface hydrophilicity of the membrane might be beneficial to enhance the cytocompatibility as previously reported.[38]

Figure 2D shows the ATR-FTIR spectra of the ESM, the ESM/DA, the ESM/HA and the ESM/KR_{600} membranes. The pristine ESM exhibited characteristic absorption peaks at 1644, 1537 and 1236 $cm,^{-1}$ which represented the amide I (C=O bond), amide II (C−N stretching vibration) and amide III (C−N stretching/N−H bending modes) bands of the proteins, respectively. Moreover, the absorption peak at 3312 cm^{-1} was assigned to the stretching mode of O−H and N−H groups.[33] After coating with polydopamine, the absorption peak approximately 3312 cm^{-1} became broader and stronger, due to the phenolic hydroxyl stretching vibration.[47] Compared with the ESM/DA, the spectrum of the ESM/HA showed stronger characteristic absorption peaks at 1644 and

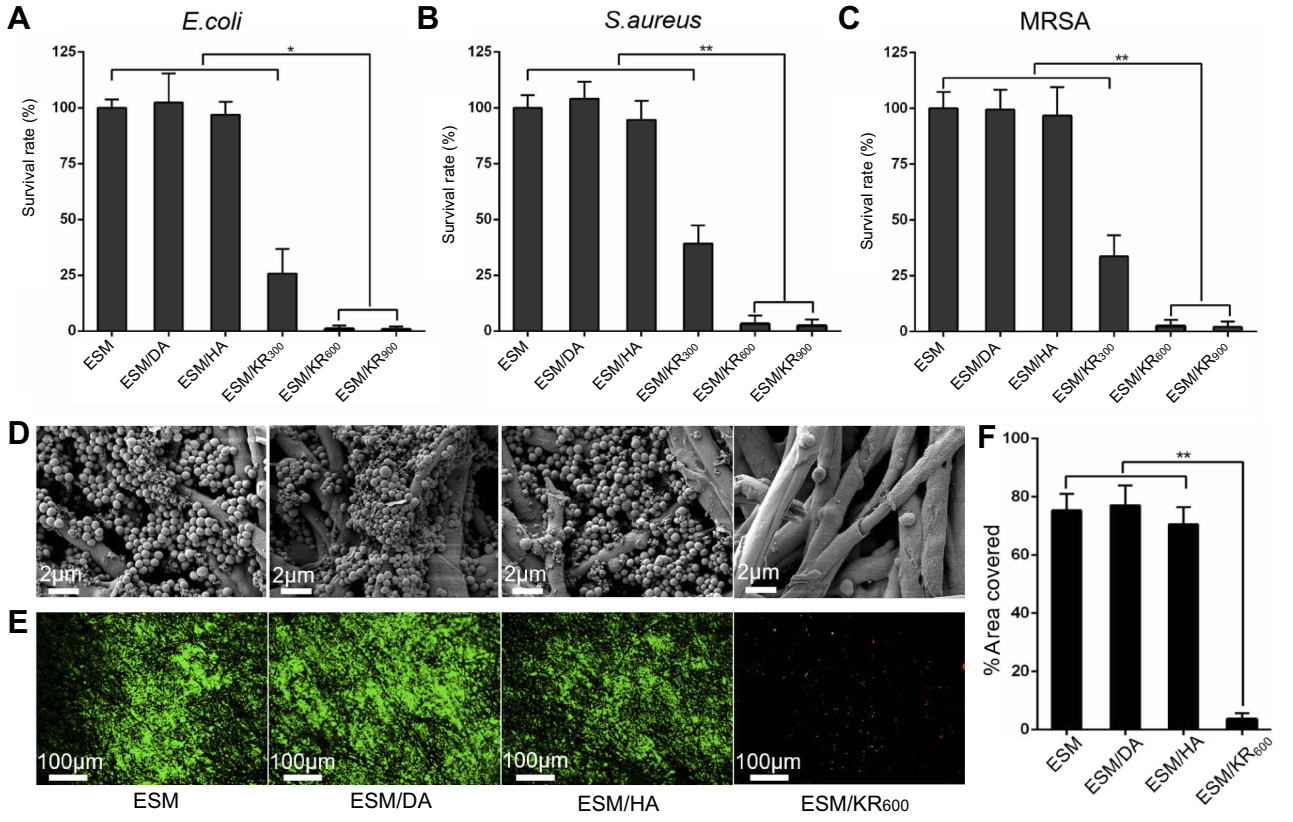

Figure 3 Antibacterial activity of the composite membranes (n=3). Bacterial viabilities of (**A**) *E. coli*, (**B**) *S. aureus* and (**C**) MRSA in different groups. (**D**) SEM images, (**E**) Live/Dead staining images and (**F**) corresponding areas of MRSA biofilm on ESM, ESM/DA, ESM/HA and ESM/KR_{600} membranes. **P*<0.05, and ***P*<0.01. **Abbreviations:** ESM, eggshell membrane; HA, hyaluronic acid; MRSA, methicillin-resistant *Staphylococcus aureus*.

1450 cm^{-1} which corresponded to C=O and C=C bonds, respectively, suggesting chemical interactions between HA and polydopamine.[48] The spectra of the ESM/HA and the ESM/KR_{600} were similar, suggesting that KR-12 peptide was immobilized on the HA coating via physical combination.

Figure 2E shows the swelling percentages of the ESM, the ESM/DA, the ESM/HA and the ESM/KR_{600} membranes. The ESM and ESM/DA membranes exhibited similar water retention ability, and their swelling percentages were 222.9% and 224.4%, respectively. However, after coating with HA, the swelling percentages of the ESM/HA and ESM/KR_{600} membranes increased to 274.2% and 269.6%, respectively, likely attributed to the visco-elastic property and hydration control ability of HA.[24,49] The improvement in the water retention capacity of the ESM/HA and the ESM/KR_{600} suggested that they could effectively absorb excess exudates from the wound, maintaining a suitable moist microenvironment for tissue regeneration.[3,50] Thus, these membranes might be applied as wound dressings.

Taken together, the results of SEM, zeta potential, water contact angle, ATR-FTIR and swelling percentage indicated that the ESM/KR-12 composite membrane (ESM/KR_{600}) was successfully prepared and expected to be used in wound treatment.

Antibacterial activities of composite membranes

The antibacterial activities of composite membranes against Gram-negative *E. coli*, and Gram-positive *S. aureus* and MRSA bacteria are shown in Figure 3A-C. Compared with pristine ESM, ESM/DA and ESM/HA, KR-12 peptide-conjugated membranes (ESM/KR_{300}, ESM/KR_{600} and ESM/KR_{900}) showed significant bactericidal activity against all three bacterial strains in a KR-12-dose-dependent manner. Specifically, the survival rates of the three bacterial strains in ESM/KR_{600} and ESM/KR_{900} groups were all less than 3%, indicating that KR-12 conjugation endowed ESM broad antibacterial activity, including the capacity to kill multi-drug-resistant bacteria. The cause might be that the positively charged KR-12 peptide immobilized on the surface of ESM could target the negatively charged bacteria via electrostatic interaction

and damage the bacterial membrane to cause membrane lysis and eventually bacterial death.[11,15]

Bacteria adhered to a biomaterial surface can grow into biofilms, which show high resistance to antibiotics and often cause persistent infection.[51,52] Thus, it is very important for a wound dressing to prevent biofilm formation. To assess the effect of as-prepared membranes on biofilm formation, the samples were co-incubated with multi-drug-resistant MRSA bacteria for 24 hrs and then were harvested for SEM analysis and the Live/Dead staining assay. As shown in Figure 3D, the surfaces of pristine ESM, ESM/DA and ESM/HA were covered by an abundant bacteria, which were grouped in large clusters and tended to grow into biofilms. However, bacteria were hardly detected growing on the surface of the ESM/KR_{600} membrane. The quantitative data also showed that the area covered by bacteria on the surface of ESM/KR_{600} was significantly less than that on the surface of other samples (Figure 3F). Moreover, Live/Dead staining images clearly revealed that the surfaces of pristine ESM, ESM/DA and ESM/HA were dominant with strong green signals (living bacteria), while only a few green signals and red signals (dead bacteria) could be observed on the surface of ESM/KR_{600} (Figure 3E), further confirming that ESM/KR_{600} was efficient to prevent the formation of MRSA biofilms. The biofilm inhibition effect of ESM/KR_{600} might be due to the mechanism that KR-12 peptide could fight against bacteria (Figure 3A-C), further preventing their adhesion and cloning on the surface of the ESM/KR_{600} membrane.[18] Collectively, KR-12 conjugated ESM/KR_{600} showed excellent bactericidal activity and anti-biofilm property and could be used as an antibacterial wound dressing.

In vitro effect of composite membranes on HUVECs

To investigate the effect of composite membranes on the proliferation of HUVECs in vitro, the cell number was first detected using the CCK-8 assay. As shown in Figure 4A, the proliferation of HUVECs in all groups exhibited an increasing profile after incubation for 1, 3 and 5 days. At day 1 post-seeding, no significant differences were observed among all groups. However, the cell viability in

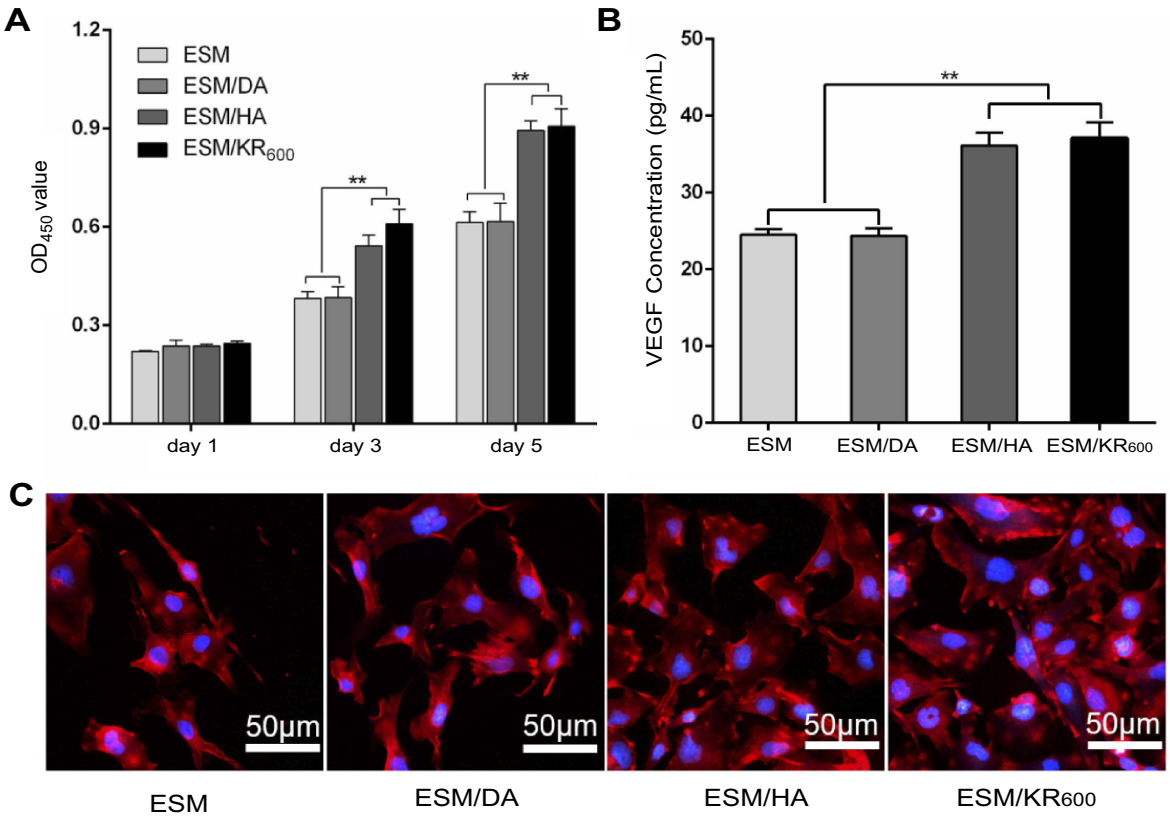

Figure 4 In vitro effects of the composite membranes on HUVECs (n=3). (**A**) OD values measured by the CCK8 assay at days 1, 3 and 5 post-seeding in different groups. (**B**) Concentration of secreted VEGF and (**C**) fluorescence images of HUVECs at day 5 post-seeding in different groups. **P<0.01.

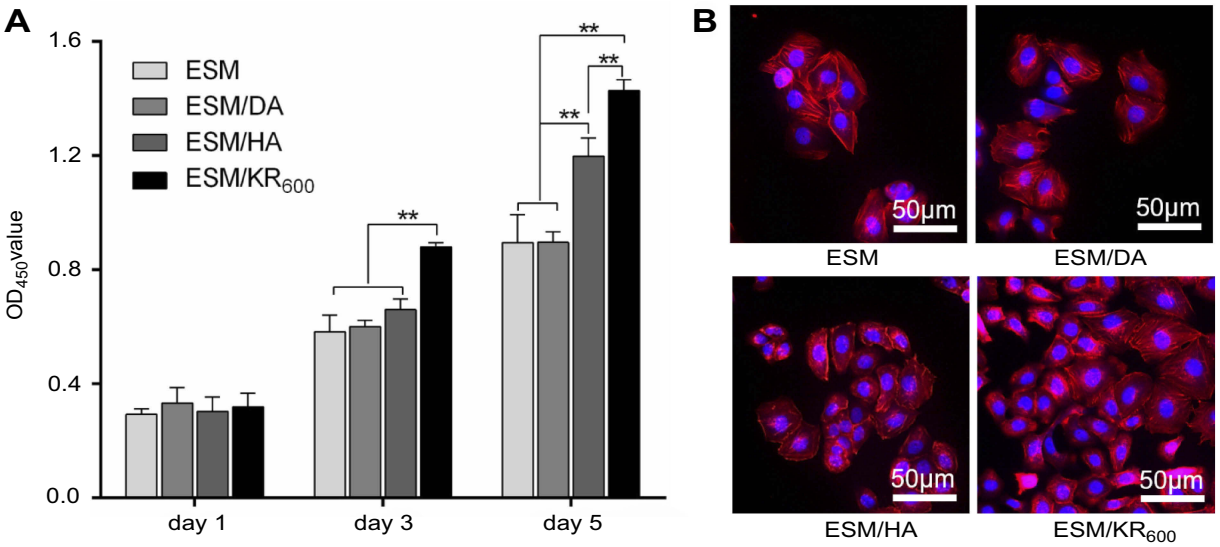

Figure 5 In vitro effects of the composite membranes on HaCaT cells (n=3). (**A**) OD values measured by the CCK8 assay at days 1, 3 and 5 post-seeding in different groups. (**B**) Fluorescence images of HaCaT cells at day 5 post-seeding in different groups. **P<0.01.

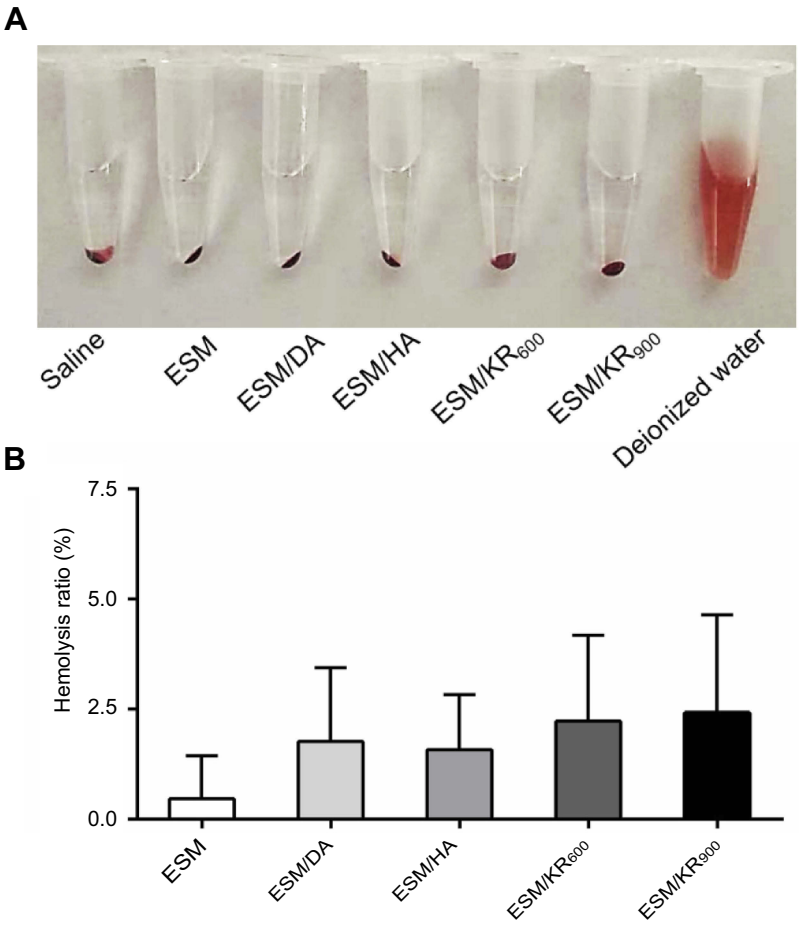

Figure 6 Blood compatibility of the composite membranes (n=3). (**A**) Images and (**B**) corresponding hemolysis ratios of fresh blood after incubation with saline, ESM, ESM/DA, ESM/HA, ESM/KR_{600}, ESM/KR_{900} and deionized water. Abbreviations: ESM, eggshell membrane; HA, hyaluronic acid.

both the ESM/HA and ESM/KR_{600} groups was significantly higher than that of the ESM and ESM/DA groups at days 3 and 5 post-seeding. Moreover, the cells after culture for 5 days were stained with phalloidin and DAPI, and the morphologies were observed under a fluorescence microscope. As shown in Figure 4C, compared with the ESM and ESM/DA groups, a larger number of cells was clearly found in the ESM/HA and ESM/KR_{600} groups. In line with the above results, the ESM/HA and ESM/KR_{600} membranes were found to increase VEGF secretion (Figure 4B), which could enhance the proliferation of HUVECs and angiogenesis.[53,54] These results suggested that the HA-coated ESM/HA and ESM/KR_{600} membranes could promote angiogenesis. According to previous reports, this might be because that HA bound to its receptor CD44 on the endothelial cell surface, on the one hand, increasing ERK and Akt phosphorylation to promote cell proliferation and VEGF expression and, on the other hand, decreasing cleaved caspase-3 expression to prevent cell apoptosis, resulting in improved HUVEC proliferation and angiogenesis.[29,30]

In vitro effect of composite membranes on HaCat cells

The effect of composite membranes on the proliferation of HaCaT cells was evaluated using the CCK8 assay and morphology observation. As presented in Figure 5, both the OD values and fluorescence images revealed that the proliferation level of HaCaT cells in the ESM/KR_{600} group was obviously higher than that in the ESM, ESM/DA and

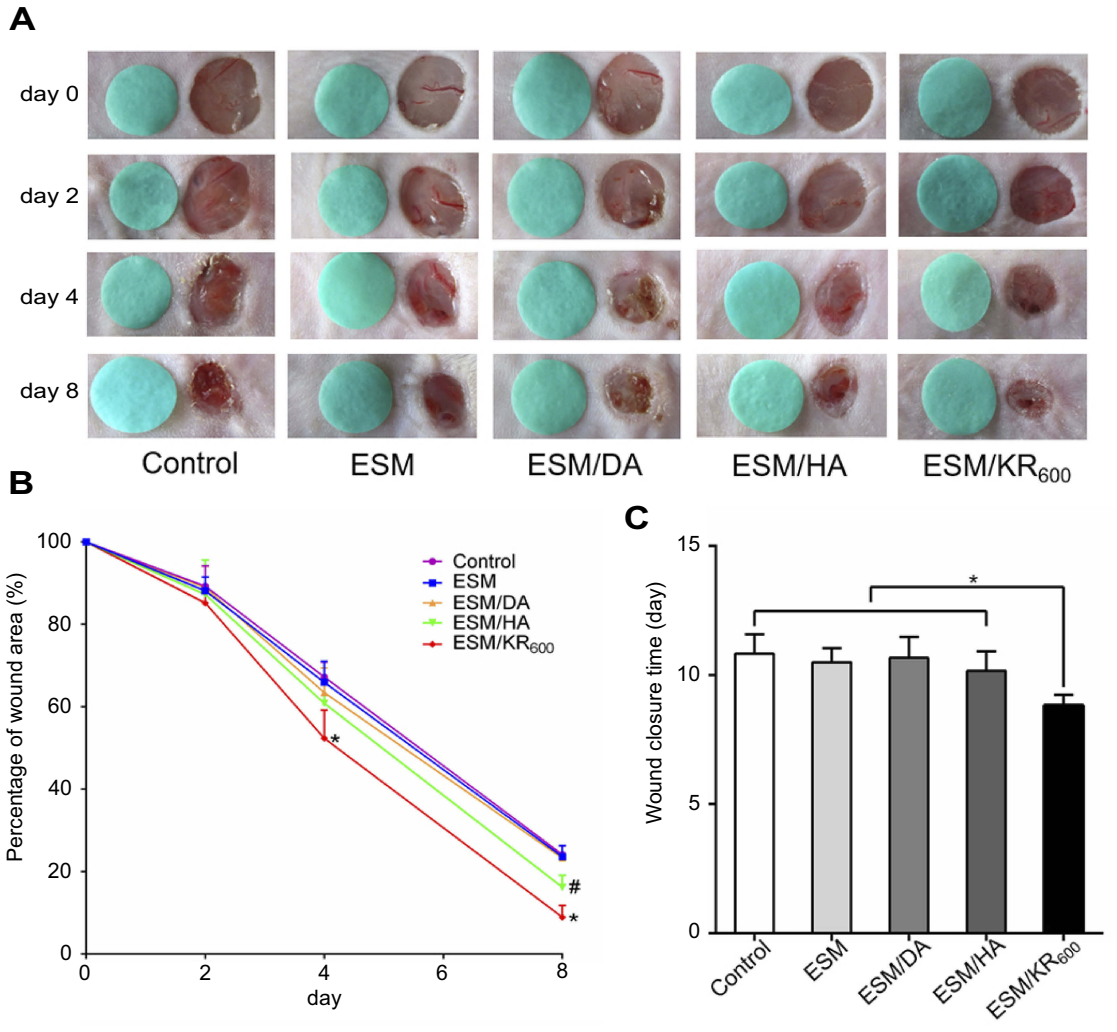

Figure 7 In vivo effects of the composite membranes on wound healing (n=5). (**A**) Images of wounds and (**B**) the corresponding percentages of wounds at determined time points. (**C**) Average complete healing times in different groups. *P<0.05 represents a significant difference between ESM/KR_{600} and other groups, while #P<0.05 represents a significant difference between the ESM/HA and ESM groups.

Abbreviations: ESM, eggshell membrane; HA, hyaluronic acid.

ESM/HA groups at days 3 and 5 post-seeding. Additionally, compared with the ESM and ESM/DA, the ESM/HA promoted the proliferation of keratinocytes at day 5 post-seeding. This result was consistent with previous studies that both HA and KR-12 peptide were helpful for the proliferation of keratinocytes, and we speculated that the ESM/KR_{600} group exhibited the highest level of cell viability likely because ESM/KR_{600} could promote keratinocyte proliferation via the synergistic effects of immobilized HA and KR-12 peptide.[19,20,28]

Hemocompatibility evaluation

The hemocompatibility of biomaterials such as wound dressings must be carefully evaluated prior to clinical use.[55] Therefore, the effect of samples on human whole blood was investigated using the hemolysis assay. As shown in Figure 6A, compared with the deionized water group, no hemolysis sign was observed in the ESM, ESM/DA, ESM/KR_{600} and ESM/KR_{900} groups. Furthermore, the quantitative data revealed that the hemolysis ratios of all membranes were below the safety threshold of 5% (Figure 6B).[42] This result indicated that KR-12 conjugated membranes had excellent hemocompatibility, which is suitable for use in wound management.

In vivo effect of composite membranes on wound healing

The wound healing performances of composite membranes were investigated using an in vivo murine wound model. The wounds were covered without a membrane (control group) or with ESM, ESM/DA, ESM/HA and ESM/KR_{600} membranes and were photographed at the determined times. Figure 7A and B displayed the macroscopic pictures of wounds and percentages of the wound area, and it was clearly observed that ESM/KR_{600} could significantly promote wound healing compared with other treatments. At day 2 post-surgery, a red and swollen sign was found around the wound in the control, ESM, ESM/DA and ESM/HA groups, but the wound treated by ESM/KR_{600} seemed to be tidy and neat, suggesting that ESM/KR_{600} might reduce the inflammation response. At day 4 and day 8 post-surgery, newly formed epidermis could be apparently observed in the wound treated by

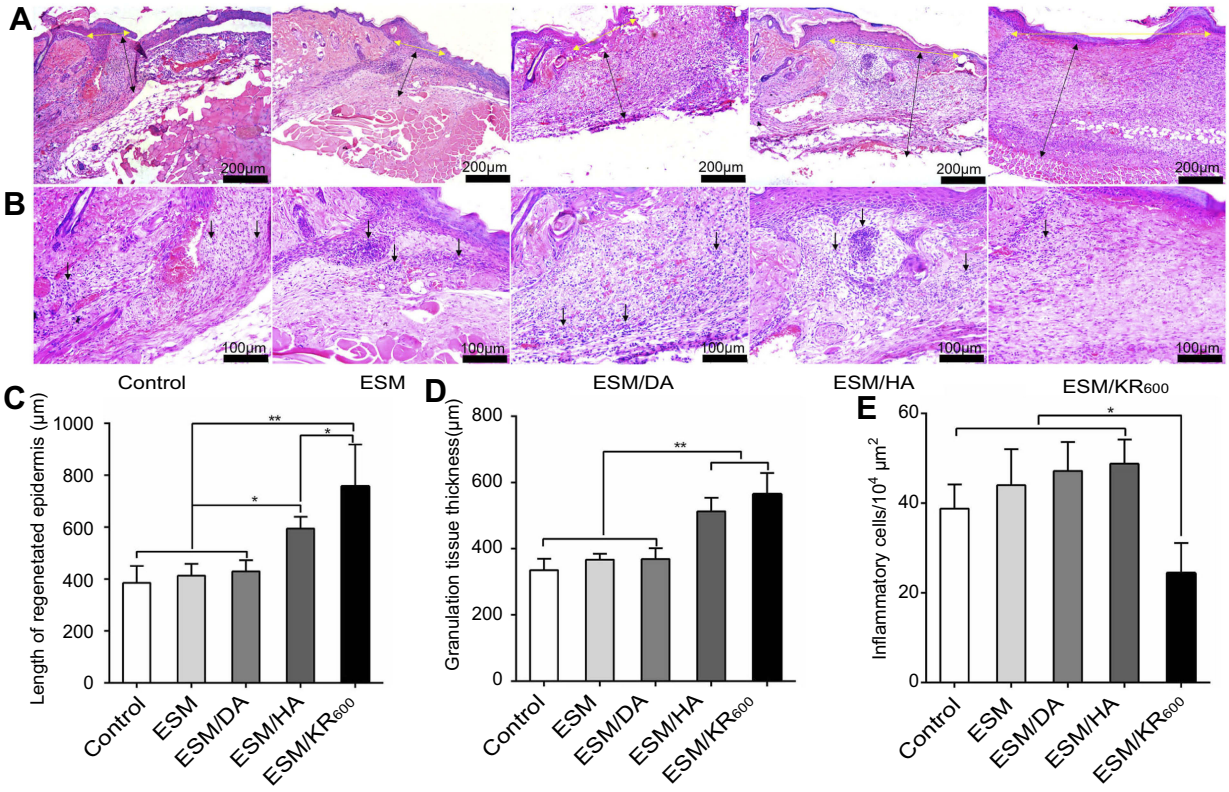

Figure 8 Histological examination of cutaneous wound sections (n=5) at day 8 post-surgery. (**A, B**) Representative H&E staining images of wound sites in different groups. The yellow double arrows indicate the regenerated epidermises, the black double arrows indicate granulation tissues and the black single arrows indicate inflammatory cells. Quantitative determination of (**C**) the length of regenerated epidermis, (**D**) thickness of granulation tissue and (**E**) number of inflammatory cells in different groups. *P<0.05 and **P<0.01.
Abbreviations: ESM, eggshell membrane; HA, hyaluronic acid.

ESM/KR_{600}, and the quantitative data revealed that the percentage of the wound area in the ESM/KR_{600} group was significantly lower than that in other groups. Particularly, at day 8 post-surgery, the percentage of the wound area in the ESM/KR_{600} group was decreased from 100.0% to 9.0%, while that in the control, ESM, ESM/DA and ESM/HA groups were 24.1%, 23.6%, 23.3% and 16.2%, respectively. ESM/HA also significantly promoted wound closure compared with pristine ESM at day 8 post-surgery, consistent with previous reports that HA contributed to wound healing.[27,28] Additionally, Figure 7C shows that the average wound closure time for the control, ESM, ESM/DA and ESM/HA groups were 10.8, 10.5, 10.7 and 10.2 days, respectively; nevertheless, it only required 8.8 days for the ESM/KR_{600}-treated mice, implying that treatment with the ESM/KR_{600} could shorten the wound closure time.

To further evaluate the efficacy of ESM/KR_{600} on wound healing, the wound tissues were collected and stained with H&E for histological examination. Re-epithelialization and granulation tissue formation as two important parameters for wound healing were first analyzed. As shown in Figure 8A and C, the length of the regenerated epidermis in the ESM/KR_{600} group was obviously longer than that in the control, ESM, ESM/DA and ESM/HA groups, indicating that ESM/KR_{600} was conducive to re-epithelialization during the wound-healing process. On the other hand, the thickness of granulation tissue in both the ESM/KR_{600} and ESM/HA groups was dramatically greater than that in the control, ESM and ESM/DA groups (Figure 8A and D), suggesting that ESM/KR_{600} and ESM/HA could promote granulation tissue formation via the beneficial effects of HA coating. Additionally, Figure 8B and E reveals that, compared

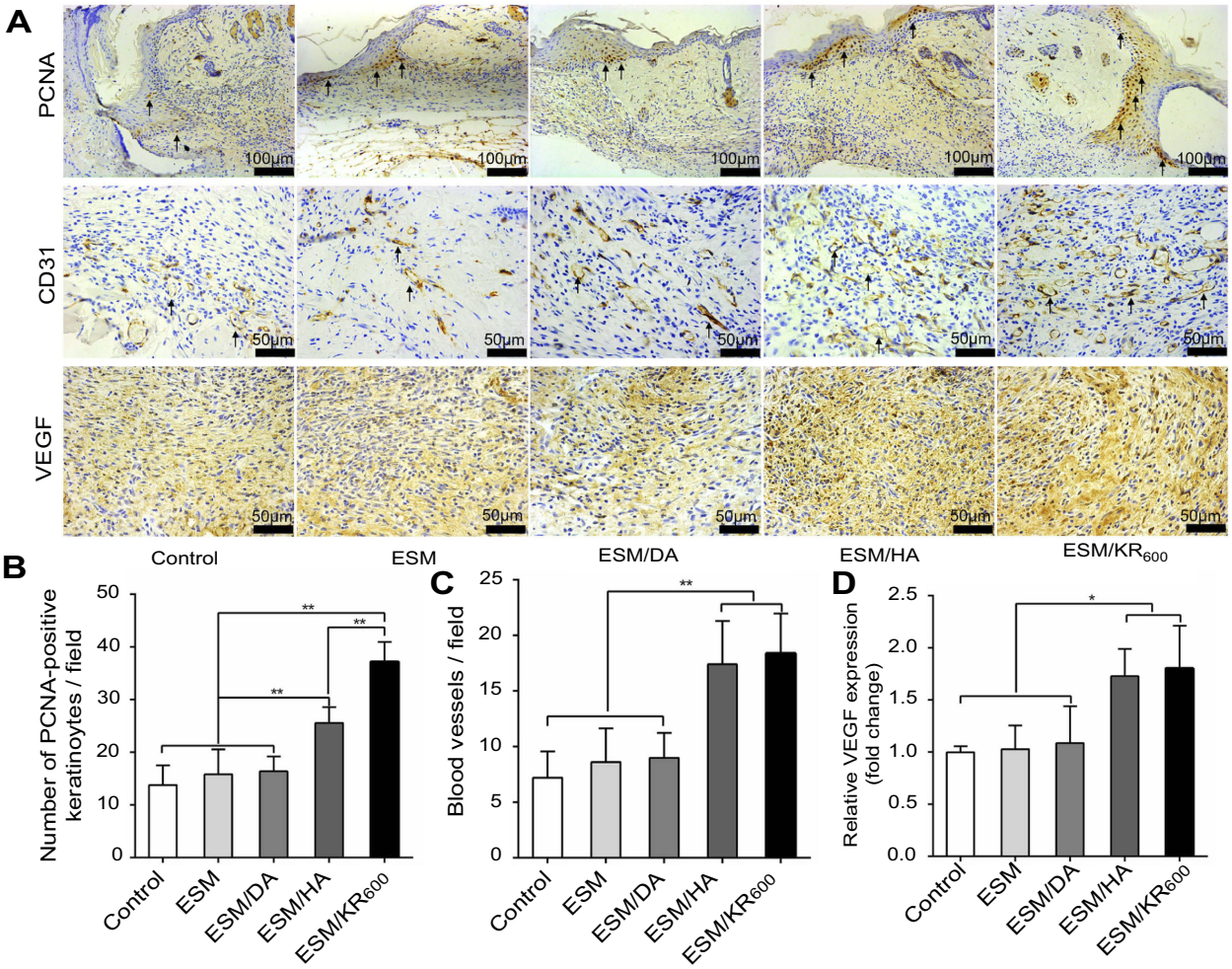

Figure 9 Immunohistochemical analysis of cutaneous wound sections (n=5) at day 8 post-surgery. (**A**) Representative images of immunohistochemical staining of PCNA, CD31 and VEGF. The black single arrows indicate PCNA-positive keratinocytes and CD-31-positive blood vessels. Quantitative counts of (**B**) PCNA-positive keratinocytes per field, (**C**) CD-31-positive blood vessels per field and (**D**) the relative expression of VEGF. *P<0.05 and **P<0.01.
Abbreviations: ESM, eggshell membrane; HA, hyaluronic acid.

with other groups, treatment with ESM/KR_{600} obviously reduced the number of inflammatory cells infiltrated to the wound edge, suggesting that ESM/KR_{600} might attenuate the inflammation reaction, as observed in the macroscopic pictures of wounds.

Thereafter, to explore the underlying mechanism of the observed phenomenon, PCNA, as a marker of cell proliferation, and CD31 and VEGF, as markers of angiogenesis, were detected using immunohistochemistry.[3,53] Figure 9A and B shows that the number of PCNA-positive keratinocytes per field in the ESM/KR_{600} group was significantly greater than that in other groups, indicating that the ESM/KR_{600} could promote keratinocyte proliferation in vivo and accelerate the re-epithelialization process, which was in line with the in vitro result (Figure 5) and previous studies that KR-12 peptide contributed to proliferation of epithelial cells.[19,20] On the other hand, Figure 9A, C and D shows that, compared with the control, ESM and ESM/DA groups, ESM/KR_{600} dramatically increased both the density of CD31-positive blood vessels and VEGF expression. However, no obvious differences were found between the ESM/KR_{600} and ESM/HA groups. In previous studies, HA had been announced to promote angiogenesis both in vitro and in vivo, through increasing endothelial cell proliferation and decreasing cell apoptosis.[29,30] Moreover, Mariarosaria et al reported that systemic administration of HA modulated angiogenesis in diabetic mice by enhancing the expression of angiogenesis-related cytokines such as TGF-β1.[31] Combined with similar in vitro results (Figure 4), we speculated that ESM/KR_{600} might improve angiogenesis mainly via the effect of HA coating, further promoting granulation tissue formation in vivo.

Taken together, ESM/KR_{600} was efficient to promote wound healing by accelerating angiogenesis and re-epithelialization in vivo, which could be attributed to the synergistic effects of KR-12 peptide and HA. Wound healing is a physiological process and is generally divided into three stages: inflammation, cell proliferation and tissue formation, and remodeling .[56] These stages overlap and interact with each other in a complex way that ultimately affects the healing process. Bacterial infection could interfere with the normal healing process and lead to delayed wound closure.[57,58] By conjugating with KR-12 peptide, ESM/KR_{600} possessed good antibacterial activity against both Gram-negative and Gram-positive bacteria, including multi-drug-resistant bacteria (Figure 3), which could effectively protect the wounds from bacterial invasion and cloning, maintaining a natural and non-septic microenvironment for new tissue formation.[1] Moreover, KR-12 peptide conjugated on ESM/KR_{600} could promote keratinocyte proliferation in vivo (Figure 9A and B) to accelerate the re-epithelialization process and cause rapid wound healing (Figures 7 and 8A). On the other hand, by coating with HA, ESM/KR_{600} could promote sufficient angiogenesis in the wound area (Figure 9A, C and D), increasing the formation of granulation tissue (Figure 8A and D). The newly generated granulation tissue could provide support for epithelial growth, further accelerating the re-epithelialization process and promoting wound closure.[54] Collectively, ESM/KR_{600} could effectively promote wound healing in vivo and potentially be an ideal wound dressing.

Conclusion

A biocompatible composite membrane composed of a polydopamine-modified ESM coated with HA and KR-12 peptide was successfully developed. The composite membrane showed excellent antibacterial activity against *E. coli, S. aureus* and multi-drug-resistant MRSA bacteria. More importantly, it could prevent the formation of a MRSA biofilm on the surface. Additionally, the composite membrane promoted the proliferation of keratinocytes and HUVECs. In vivo animal testing showed that the composite membrane accelerated re-epithelialization via promoting keratinocyte proliferation and enhanced granulation tissue formation via promoting angiogenesis, eventually leading to rapid wound healing. Therefore, the prepared composite membrane is a promising dressing for wound treatment.

Acknowledgments

This work was supported by the National Special Scientific Projects of Public Welfare Industry Funding of China (No. 201502015) and State Key Laboratory Funding (SKLZZ201221).

Disclosure

The authors report no conflicts of interest in this work.

References

1. Mogosanu GD, Grumezescu AM. Natural and synthetic polymers for wounds and burns dressing. *Int J Pharm*. 2014;463:127–136. doi:10.1016/j.ijpharm.2013.12.015
2. Sarhan WA, Azzazy HM, El-Sherbiny IM. Honey/chitosan nanofiber wound dressing enriched with allium sativum and cleome droserifolia: enhanced antimicrobial and wound healing activity. *ACS Appl Mater Interfaces*. 2016;8:6379–6390. doi:10.1021/acsami.6b00739
3. Xu R, Luo G, Xia H, et al. Novel bilayer wound dressing composed of silicone rubber with particular micropores enhanced wound re-epithelialization and contraction. *Biomaterials*. 2015;40:1–11. doi:10.1016/j.biomaterials.2014.10.077

4. Aguirre A, Gonzalez A, Navarro M, Castano O, Planell JA, Engel E. Control of microenvironmental cues with a smart biomaterial composite promotes endothelial progenitor cell angiogenesis. *Eur Cell Mater*. 2012;24:90–106.
5. Soller EC, Tzeranis DS, Miu K, So PT, Yannas IV. Common features of optimal collagen scaffolds that disrupt wound contraction and enhance regeneration both in peripheral nerves and in skin. *Biomaterials*. 2012;33:4783–4791. doi:10.1016/j.biomaterials.2012.03.068
6. Popat KC, Eltgroth M, Latempa TJ, Grimes CA, Desai TA. Decreased staphylococcus epidermis adhesion and increased osteoblast functionality on antibiotic-loaded titania nanotubes. *Biomaterials*. 2007;28:4880–4888. doi:10.1016/j.biomaterials.2007.07.037
7. Ye S, Jiang L, Wu J, et al. Flexible amoxicillin grafted bacterial cellulose sponges for wound dressing: in vitro and in vivo evaluation. *ACS Appl Mater Interfaces*. 2018;10:5862–5870. doi:10.1021/acsami.7b16680
8. World Health Organization fact sheet - antibiotic resistance. 2018; Available from: http://www.who.int/news-room/fact-sheets/detail/antibiotic-resistance. Accessed May 08, 2018.
9. Majumder P, Bhunia S, Chaudhuri A. A lipid-based cell penetrating nano-assembly for RNAi-mediated anti-angiogenic cancer therapy. *Chem Commun*. 2018;54(12):1489–1492. doi:10.1039/C7CC08517F
10. Majumder P, Bhunia S, Bhattacharyya J, Chaudhuri A. Inhibiting tumor growth by targeting liposomally encapsulated CDC20siRNA to tumor vasculature: therapeutic RNA interference. *J Control Release*. 2014;180:100–108. doi:10.1016/j.jconrel.2014.02.012
11. Hancock RE, Sahl HG. Antimicrobial and host-defense peptides as new anti-infective therapeutic strategies. *Nat Biotechnol*. 2006;24:1551–1557. doi:10.1038/nbt1267
12. Peng LH, Huang YF, Zhang CZ, et al. Integration of antimicrobial peptides with gold nanoparticles as unique non-viral vectors for gene delivery to mesenchymal stem cells with antibacterial activity. *Biomaterials*. 2016;103:137–149. doi:10.1016/j.biomaterials.2016.06.057
13. Han J, Zhao S, Ma Z, et al. The antibacterial activity and modes of LI-F type antimicrobial peptides against bacillus cereus in vitro. *J Appl Microbiol*. 2017;123:602–614. doi:10.1111/jam.13526
14. Domalaon R, Zhanel GG, Schweizer F. Short antimicrobial peptides and peptide scaffolds as promising antibacterial agents. *Curr Top Med Chem*. 2016;16:1217–1230.
15. Shai Y. Mode of action of membrane active antimicrobial peptides. *Biopolymers*. 2002;66:236–248. doi:10.1002/bip.10260
16. Nagy K, Mikulass KR, Vegh AG, et al. Interaction of cysteine-rich cationic antimicrobial peptides with intact bacteria and model membranes. *Gen Physiol Biophys*. 2015;34:135–144. doi:10.4149/gpb_2015002
17. Wang G. Structures of human host defense cathelicidin LL-37 and its smallest antimicrobial peptide KR-12 in lipid micelles. *J Biol Chem*. 2008;283:32637–32643. doi:10.1074/jbc.M805533200
18. Jacob B, Park IS, Bang JK, Shin SY. Short KR-12 analogs designed from human cathelicidin LL-37 possessing both antimicrobial and antiendotoxic activities without mammalian cell toxicity. *J Pept Sci*. 2013;19:700–707. doi:10.1002/psc.2552
19. Carretero M, Escamez MJ, Garcia M, et al. In vitro and in vivo wound healing-promoting activities of human cathelicidin LL-37. *J Invest Dermatol*. 2008;128:223–236. doi:10.1038/sj.jid.5701043
20. Song DW, Kim SH, Kim HH, Lee KH, Ki CS, Park YH. Multi-biofunction of antimicrobial peptide-immobilized silk fibroin nanofiber membrane: implications for wound healing. *Acta Biomater*. 2016;39:146–155. doi:10.1016/j.actbio.2016.05.008
21. Gao G, Lange D, Hilpert K, et al. The biocompatibility and biofilm resistance of implant coatings based on hydrophilic polymer brushes conjugated with antimicrobial peptides. *Biomaterials*. 2011;32:3899–3909. doi:10.1016/j.biomaterials.2011.02.013
22. Gorustovich AA, Roether JA, Boccaccini AR. Effect of bioactive glasses on angiogenesis: a review of in vitro and in vivo evidences. *Tissue Eng Part B Rev*. 2010;16:199–207. doi:10.1089/ten.TEB.2009.0416
23. Segura T, Anderson BC, Chung PH, Webber RE, Shull KR, Shea LD. Crosslinked hyaluronic acid hydrogels: a strategy to functionalize and pattern. *Biomaterials*. 2005;26:359–371. doi:10.1016/j.biomaterials.2004.02.067
24. Burdick JA, Prestwich GD. Hyaluronic acid hydrogels for biomedical applications. *Adv Mater*. 2011;23:41–56. doi:10.1002/adma.201003963
25. Meyer K. Chemical structure of hyaluronic acid. *Fed Proc*. 1958;17:1075–1077.
26. Hanci D, Altun H. Effectiveness of hyaluronic acid in post-tonsillectomy pain relief and wound healing: a prospective, double-blind, controlled clinical study. *Int J Pediatr Otorhinolaryngol*. 2015;79:1388–1392. doi:10.1016/j.ijporl.2015.07.016
27. Chen WY, Abatangelo G. Functions of hyaluronan in wound repair. *Wound Repair Regen*. 1999;7:79–89.
28. Bourguignon LY. Matrix hyaluronan-activated CD44 signaling promotes keratinocyte activities and improves abnormal epidermal functions. *Am J Pathol*. 2014;184:1912–1919. doi:10.1016/j.ajpath.2014.03.010
29. Tang ZC, Liao WY, Tang AC, Tsai SJ, Hsieh PC. The enhancement of endothelial cell therapy for angiogenesis in hindlimb ischemia using hyaluronan. *Biomaterials*. 2011;32:75–86. doi:10.1016/j.biomaterials.2010.08.085
30. Huang L, Wang Y, Liu H, Huang J. Local injection of high-molecular hyaluronan promotes wound healing in old rats by increasing angiogenesis. *Oncotarget*. 2018;9:8241–8252. doi:10.18632/oncotarget.23246
31. Galeano M, Polito F, Bitto A, et al. Systemic administration of high-molecular weight hyaluronan stimulates wound healing in genetically diabetic mice. *Biochim Biophys Acta*. 2011;1812:752–759. doi:10.1016/j.bbadis.2011.03.012
32. Toole BP, Wight TN, Tammi MI. Hyaluronan-cell interactions in cancer and vascular disease. *J Biol Chem*. 2002;277:4593–4596. doi:10.1074/jbc.R100039200
33. Balaz M. Eggshell membrane biomaterial as a platform for applications in materials science. *Acta Biomater*. 2014;10:3827–3843. doi:10.1016/j.actbio.2014.03.020
34. Ahlborn GJ, Clare DA, Sheldon BW, Kelly RW. Identification of eggshell membrane proteins and purification of ovotransferrin and beta-NAGase from hen egg white. *Protein J*. 2006;25:71–81. doi:10.1007/s10930-006-0010-8
35. Ray PG, Roy S. Eggshell membrane: a natural substrate for immobilization and detection of DNA. *Mater Sci Eng C Mater Biol Appl*. 2016;59:404–410. doi:10.1016/j.msec.2015.10.034
36. Yang JY, Chuang SS, Yang WG, Tsay PK. Egg membrane as a new biological dressing in split-thickness skin graft donor sites: a preliminary clinical evaluation. *Chang Gung Med J*. 2003;26:153–159.
37. Ohto-Fujita E, Konno T, Shimizu M, et al. Hydrolyzed eggshell membrane immobilized on phosphorylcholine polymer supplies extracellular matrix environment for human dermal fibroblasts. *Cell Tissue Res*. 2011;345:177–190. doi:10.1007/s00441-011-1172-z
38. Madhurakkat Perikamana SK, Lee J, Lee YB, et al. Materials from mussel-inspired chemistry for cell and tissue engineering applications. *Biomacromolecules*. 2015;16:2541–2555. doi:10.1021/acs.biomac.5b00852
39. Lee H, Dellatore SM, Miller WM, Messersmith PB. Mussel-inspired surface chemistry for multifunctional coatings. *Science*. 2007;318:426–430. doi:10.1126/science.1147241
40. Croisier F, Atanasova G, Poumay Y, Jerome C. Polysaccharide-coated PCL nanofibers for wound dressing applications. *Adv Healthc Mater*. 2014;3:2032–2039. doi:10.1002/adhm.201400380
41. Liu M, Luo G, Wang Y, et al. Optimization and integration of nanosilver on polycaprolactone nanofibrous mesh for bacterial inhibition and wound healing in vitro and in vivo. *Int J Nanomed*. 2017;12:6827–6840. doi:10.2147/IJN.S140648

42. Wang J, Hu W, Liu Q, Zhang S. Dual-functional composite with anticoagulant and antibacterial properties based on heparinized silk fibroin and chitosan. *Colloid Surface B*. 2011;85:241–247. doi:10.1016/j.colsurfb.2011.02.035
43. Wang Y, Xu R, Luo G, et al. Biomimetic fibroblast-loaded artificial dermis with "sandwich" structure and designed gradient pore sizes promotes wound healing by favoring granulation tissue formation and wound re-epithelialization. *Acta Biomater*. 2016;30:246–257. doi:10.1016/j.actbio.2015.11.035
44. Leguen E, Chassepot A, Decher G, Schaaf P, Voegel JC, Jessel N. Bioactive coatings based on polyelectrolyte multilayer architectures functionalized by embedded proteins, peptides or drugs. *Biomol Eng*. 2007;24:33–41. doi:10.1016/j.bioeng.2006.05.023
45. Ku SH, Park CB. Myoblast differentiation on graphene oxide. *Biomaterials*. 2013;34:2017–2023. doi:10.1016/j.biomaterials.2012.11.052
46. Hilpert K, Elliott M, Jenssen H, et al. Screening and characterization of surface-tethered cationic peptides for antimicrobial activity. *Chem Biol*. 2009;16:58–69. doi:10.1016/j.chembiol.2008.11.006
47. Jia Z, Xiu P, Li M, et al. Bioinspired anchoring AgNPs onto micro-nanoporous TiO2 orthopedic coatings: trap-killing of bacteria, surface-regulated osteoblast functions and host responses. *Biomaterials*. 2016;75:203–222. doi:10.1016/j.biomaterials.2015.10.035
48. Lu B, Lu F, Zou Y, et al. In situ reduction of silver nanoparticles by chitosan-l-glutamic acid/hyaluronic acid: enhancing antimicrobial and wound-healing activity. *Carbohydr Polym*. 2017;173:556–565. doi:10.1016/j.carbpol.2017.06.035
49. Laurent TC, Laurent UB, Fraser JR. Functions of hyaluronan. *Ann Rheum Dis*. 1995;54:429–432.
50. GhavamiNejad A, Rajan UA, Ramachandra Kurup Sasikala A, et al. Mussel-inspired electrospun nanofibers functionalized with size-controlled silver nanoparticles for wound dressing application. *ACS Appl Mater Interfaces*. 2015;7:12176–12183. doi:10.1021/acsami.5b02542
51. Flemming HC, Wingender J. The biofilm matrix. *Nat Rev Microbiol*. 2010;8:623–633. doi:10.1038/nrmicro2415
52. Ivanova K, Fernandes MM, Francesko A, et al. Quorum-quenching and matrix-degrading enzymes in multilayer coatings synergistically prevent bacterial biofilm formation on urinary catheters. *ACS Appl Mater Interfaces*. 2015;7:27066–27077. doi:10.1021/acsami.5b09489
53. Law AY, Wong CK. Stanniocalcin-1 and −2 promote angiogenic sprouting in HUVECs via vegf/vegfr2 and angiopoietin signaling pathways. *Mol Cell Endocrinol*. 2013;374:73–81. doi:10.1016/j.mce.2013.04.024
54. Yang HS, Shin J, Bhang SH, et al. Enhanced skin wound healing by a sustained release of growth factors contained in platelet-rich plasma. *Exp Mol Med*. 2011;43:622–629. doi:10.3858/emm.2011.43.11.070
55. Dobrovolskaia MA, Clogston JD, Neun BW, Hall JB, Patri AK, McNeil SE. Method for analysis of nanoparticle hemolytic properties in vitro. *Nano Lett*. 2008;8:2180–2187. doi:10.1021/nl0805615
56. Gurtner GC, Werner S, Barrandon Y, Longaker MT. Wound repair and regeneration. *Nature*. 2008;453:314–321. doi:10.1038/nature07039
57. Percival SL, McCarty SM. Silver and alginates: role in wound healing and biofilm control. *Adv Wound Care (New Rochelle)*. 2015;4:407–414. doi:10.1089/wound.2014.0541
58. Liu T, Liu Y, Liu M, et al. Synthesis of graphene oxide-quaternary ammonium nanocomposite with synergistic antibacterial activity to promote infected wound healing. *Burns Trauma*. 2018;6:1–23. doi:10.1186/s41038-017-0106-8

International Journal of Nanomedicine Dovepress

Publish your work in this journal

The International Journal of Nanomedicine is an international, peer-reviewed journal focusing on the application of nanotechnology in diagnostics, therapeutics, and drug delivery systems throughout the biomedical field. This journal is indexed on PubMed Central, MedLine, CAS, SciSearch®, Current Contents®/Clinical Medicine, Journal Citation Reports/Science Edition, EMBase, Scopus and the Elsevier Bibliographic databases. The manuscript management system is completely online and includes a very quick and fair peer-review system, which is all easy to use. Visit http://www.dovepress.com/testimonials.php to read real quotes from published authors.

Submit your manuscript here: https://www.dovepress.com/international-journal-of-nanomedicine-journal